The Coulomb gauge model

Felipe J. Llanes-Estrada

fllanes@fis.ucm.es

U. Complutense Madrid

QCD in Coulomb gauge

$$H = \int \left[\frac{1}{2} \mathcal{J}^{-1} \mathbf{E}_a^{tr} \mathcal{J} \mathbf{E}^{a\,tr} + \frac{1}{2} \mathbf{B}^a \mathbf{B}_a \right]$$

$$+ \int \overline{\Psi} [\gamma \cdot (\nabla - i g_0 T^a \mathbf{A}_a) + m] \Psi d\mathbf{x}$$

$$+ \frac{1}{2} g_0^2 \int \int \mathcal{J}^{-1} \rho^a(\mathbf{x}) v(|\mathbf{x} - \mathbf{y}|)_{aa'} \mathcal{J} \rho^{a'}(\mathbf{y}) d\mathbf{x} d\mathbf{y}$$

Color density and current:

$$\begin{aligned} \rho^a(\boldsymbol{x}) &= \Psi^\dagger(\boldsymbol{x}) T^a \Psi(\boldsymbol{x}) + f^{abc} \mathbf{A}^b(\boldsymbol{x}) \cdot \mathbf{\Pi}^c(\boldsymbol{x}) \\ \mathbf{J}^a &= \Psi^\dagger(\boldsymbol{x}) \boldsymbol{\alpha} T^a \Psi(\boldsymbol{x}) \end{aligned}$$

Lattice static potential

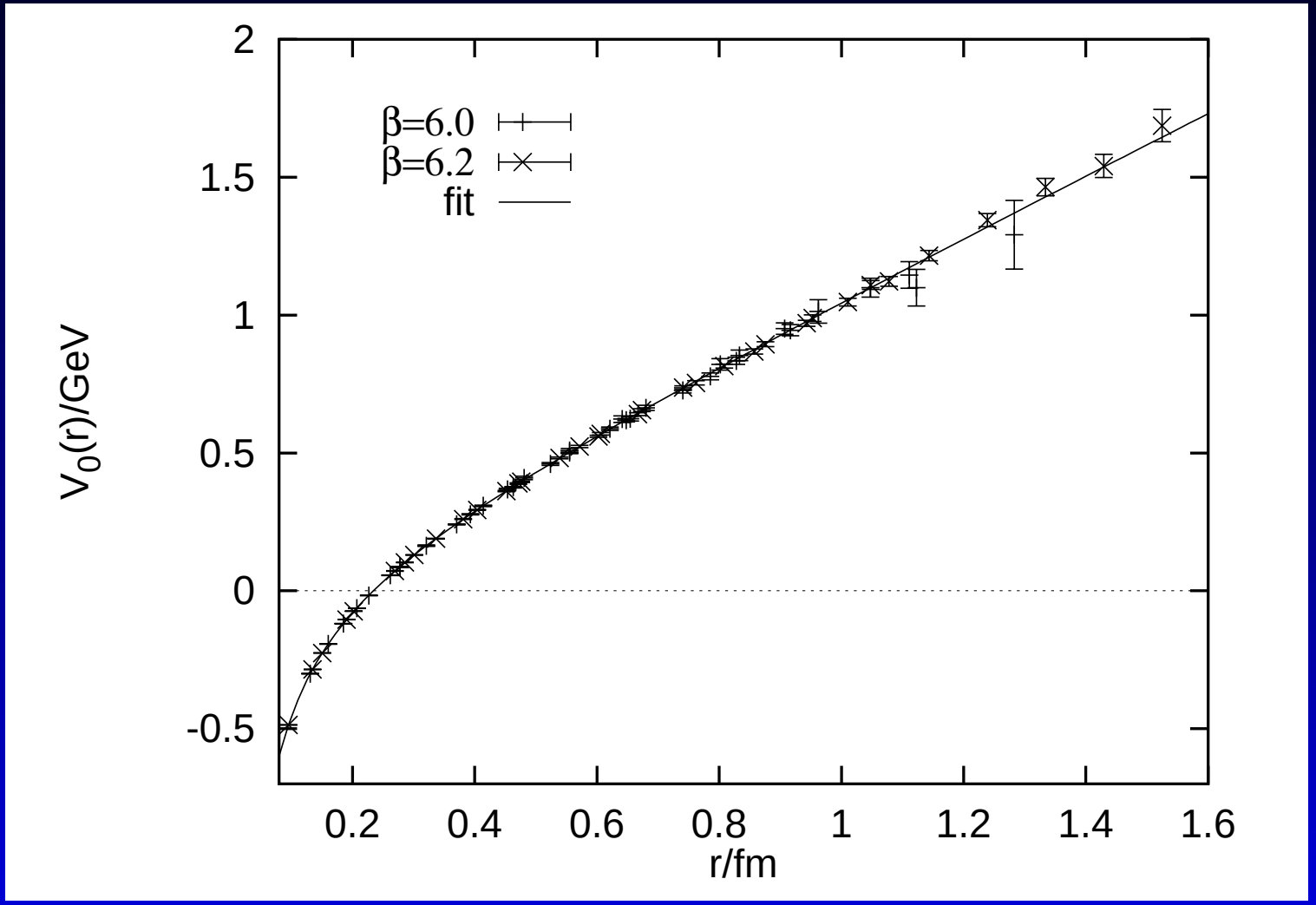

Bali and Schilling, PRD1997

Coulomb gauge model

Upgrade of the Cornell potential model to field theory

$$H = -g_s \int d\mathbf{x} \Psi^\dagger(x) \alpha \cdot \mathbf{A}(x) \Psi(x)$$

$$+Tr \int d\mathbf{x} (\mathbf{E}\cdot\mathbf{E} + \mathbf{B}\cdot\mathbf{B})$$

$$+ \int d\mathbf{x} \Psi_q^\dagger(\mathbf{x}) (-i\alpha\cdot\nabla + \beta m_q) \Psi_q(\mathbf{x})$$

$$-\frac{1}{2} \int d\mathbf{x} d\mathbf{y} \rho^a(\mathbf{x}) V_L(|\mathbf{x}-\mathbf{y}|) \rho^a(\mathbf{y})$$

BCS angle and spinors

$$\sin\phi(k) \equiv \frac{M(k)}{\sqrt{M(k)^2+k^2}}$$

$$U_{\kappa\lambda} = \frac{1}{\sqrt{2}}\begin{bmatrix} \sqrt{1+\sin\phi_\kappa}\chi_\lambda \\ \sqrt{1-\sin\phi_\kappa}\vec{\sigma}\cdot\hat{\kappa}\chi_\lambda \end{bmatrix}$$

$$V_{-\kappa\lambda} = \frac{1}{\sqrt{2}}\begin{bmatrix} -\sqrt{1-\sin\phi_\kappa}\vec{\sigma}\cdot\hat{\kappa}i\sigma_2\chi_\lambda \\ \sqrt{1+\sin\phi_\kappa}i\sigma_2\chi_\lambda \end{bmatrix}.$$

BCS gap equation

$$|\Omega\rangle = \exp\left(-\sum_{\lambda i}\int \frac{d\mathbf{k}}{(2\pi)^3}\lambda \tan\frac{\theta_k}{2} b^\dagger_{\mathbf{k}\lambda i} d^\dagger_{-\mathbf{k}\lambda i}\right)|0\rangle \quad (1)$$

$$\begin{aligned} k s_k - m c_k = & \frac{2}{3}\int \frac{d\boldsymbol{q}}{(2\pi)^3}\left[(s_k c_q x - s_q c_k)V(|\boldsymbol{k}-\boldsymbol{q}|)\right. \\ - & \left. 2c_k s_q U(|\boldsymbol{k}-\boldsymbol{q}|) + 2c_q s_k W(|\boldsymbol{k}-\boldsymbol{q}|)\right] \end{aligned}$$

Adler and Davis NPB1984; Le Yaouanc et al PRD1986;

Bicudo and Ribeiro PRD1989

Mass gap generation

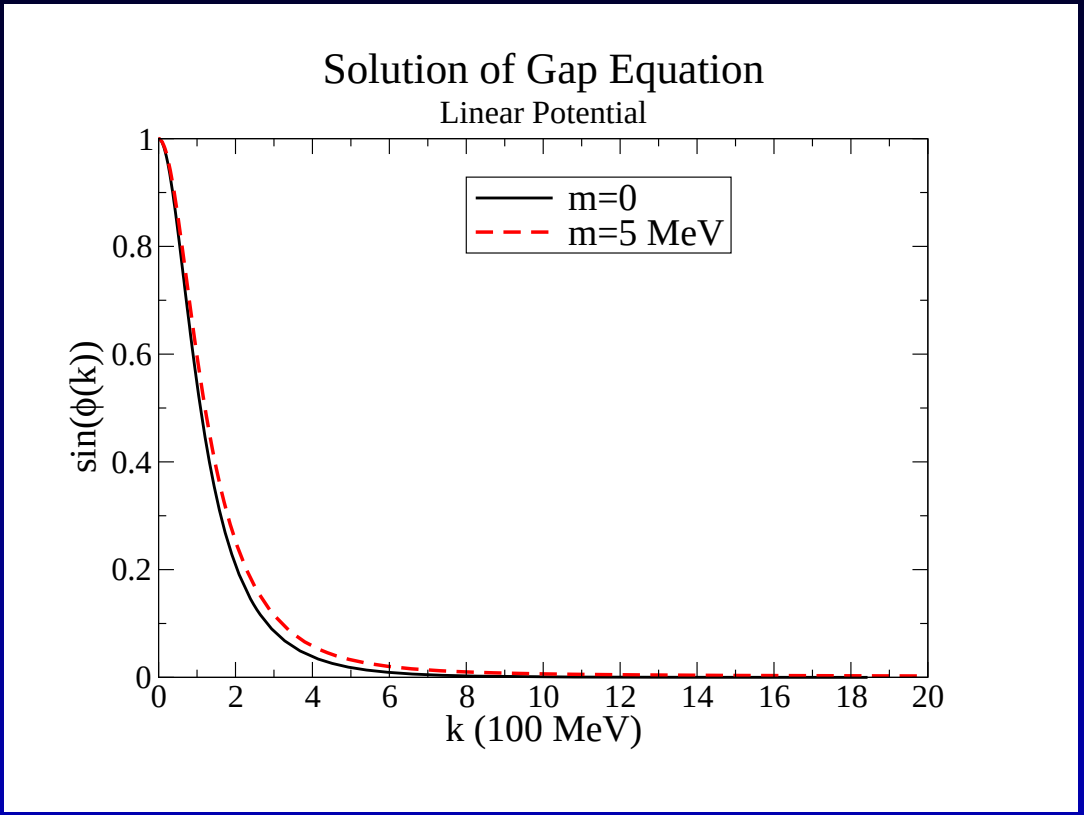

Mexican hat

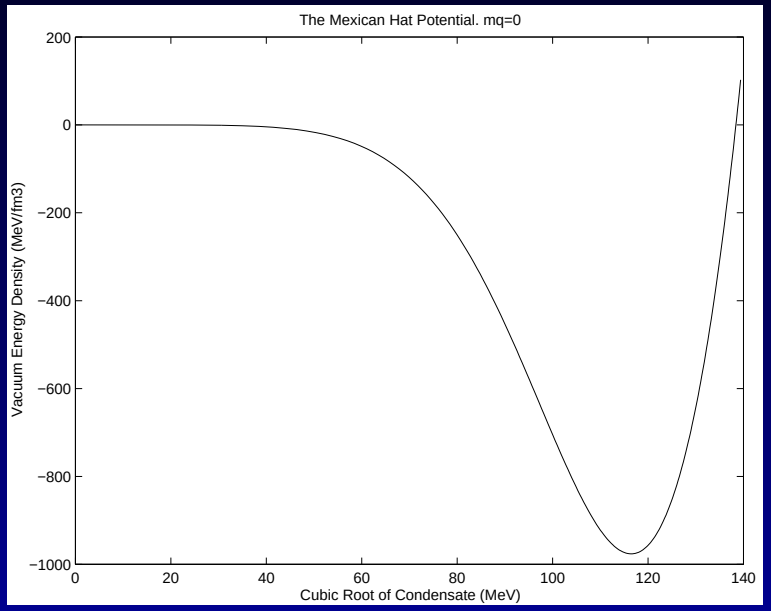
The Mexican Hat Potential. mq=0
Vacuum Energy Density (MeV/fm3)
Cubic Root of Condensate (MeV)
200
0
−200
−400
−600
−800
−1000
0
20
40
60
80
100
120
140

Gluon gap equation

$$|\Omega\rangle = \exp \int \frac{d\mathbf{k}}{(2\pi)^3}\frac{1}{2}\tanh\theta_k(\hat{k}_i\hat{k}_j-\delta_{ij})a_i^{\dagger a}(\mathbf{k})a_{ja}^{\dagger}(-\mathbf{k})$$

$$\omega_k^2 = k^2-\frac{3}{4}\int \frac{d\mathbf{q}}{(2\pi)^3}\hat{V}(|\mathbf{k}-\mathbf{q}|)(1+(\hat{k}\cdot\hat{q})^2)\left(\frac{w_q^2-w_k^2}{w_q}\right.$$

Szczepaniak, Swanson, Ji and Cotanch PRL96

Mass gap generation

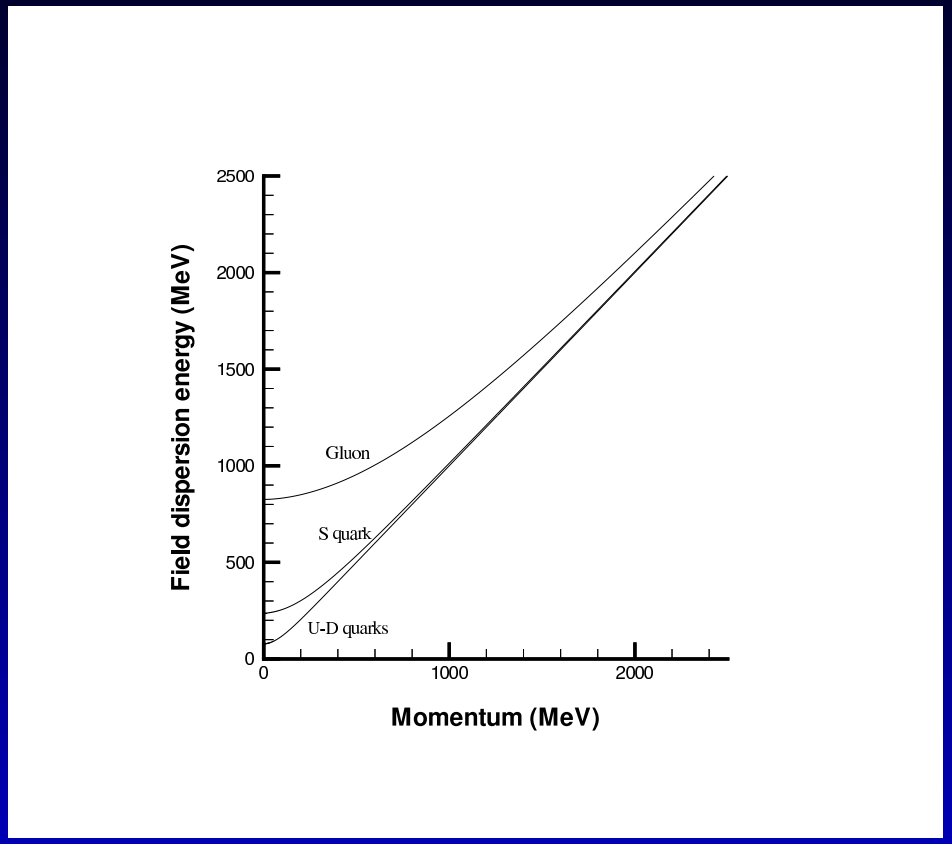

Mesons in Tamm-Dancoff

$$|G\rangle = \int \frac{d\mathbf{q}}{(2\pi)^3} \sum_{a\mu\nu} \phi^{(n)}_{\mu\nu}(\mathbf{q}) \alpha^{a\dagger}_{\mu}(\mathbf{q}) \alpha^{a\dagger}_{\nu}(-\mathbf{q}) |\Omega\rangle \ .$$

$$|Q\bar{Q}\rangle = \sum_{\gamma\delta} \Psi^{*n}_{\gamma\delta} B^{\dagger}_{\gamma} D^{\dagger}_{\delta} |\Omega\rangle_{BCS}$$

Cotanch and Ll-E NPA2002

Light meson spectrum

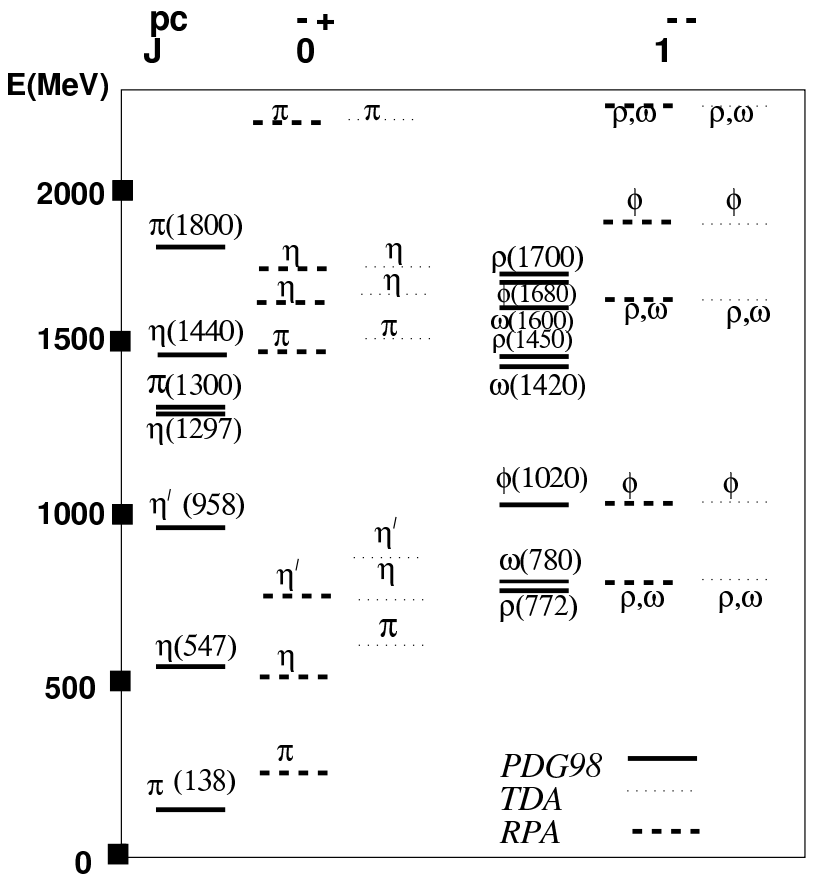

Light meson spectrum

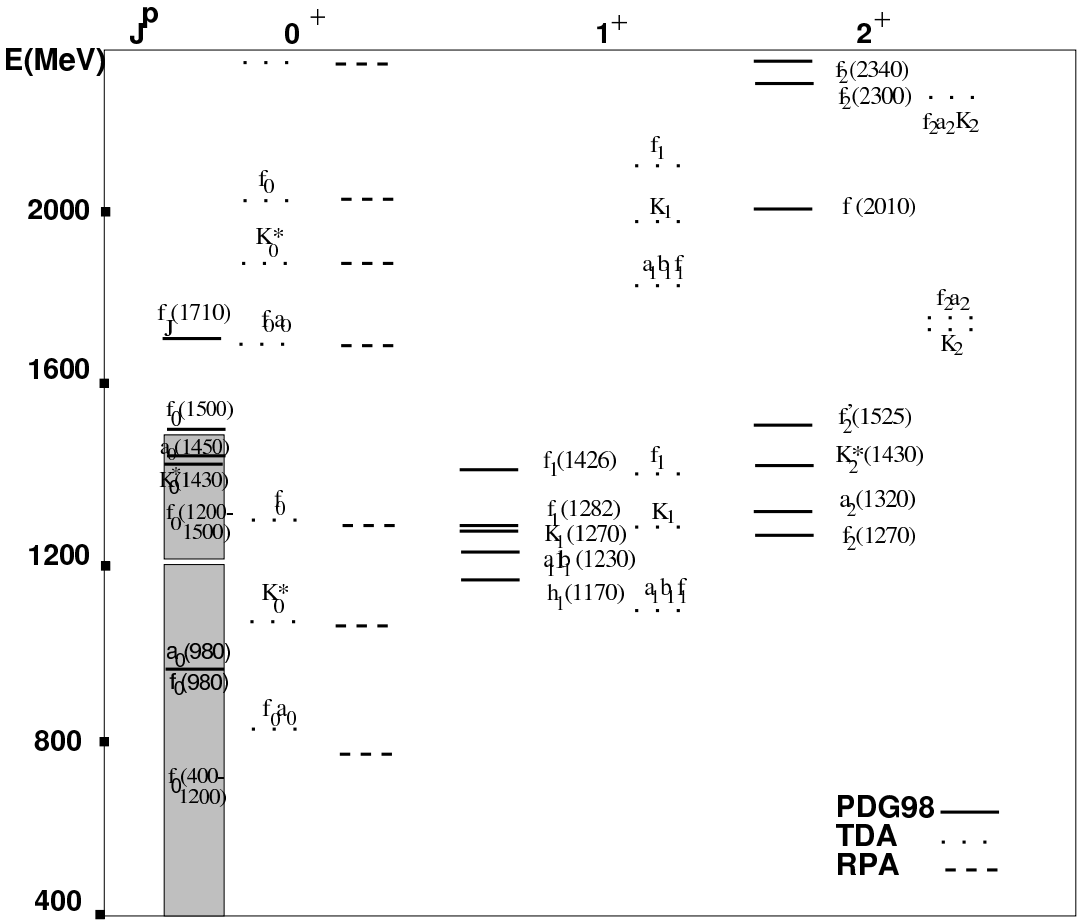

RPA: Gell-Mann-Oakes-Renner

Llanes-Estrada and Cotanch, PRL 2000

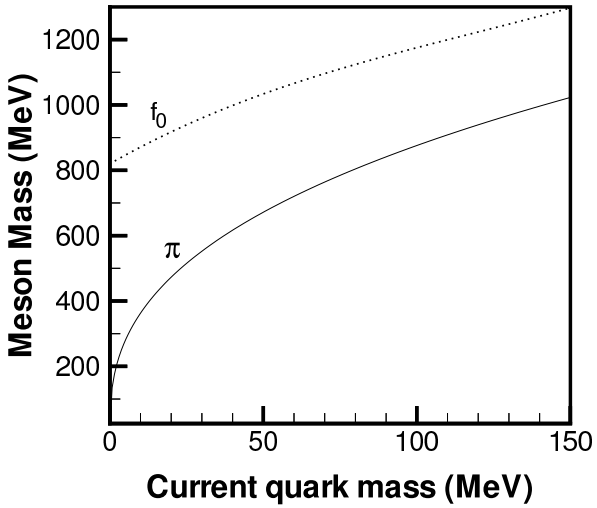

D spectrum

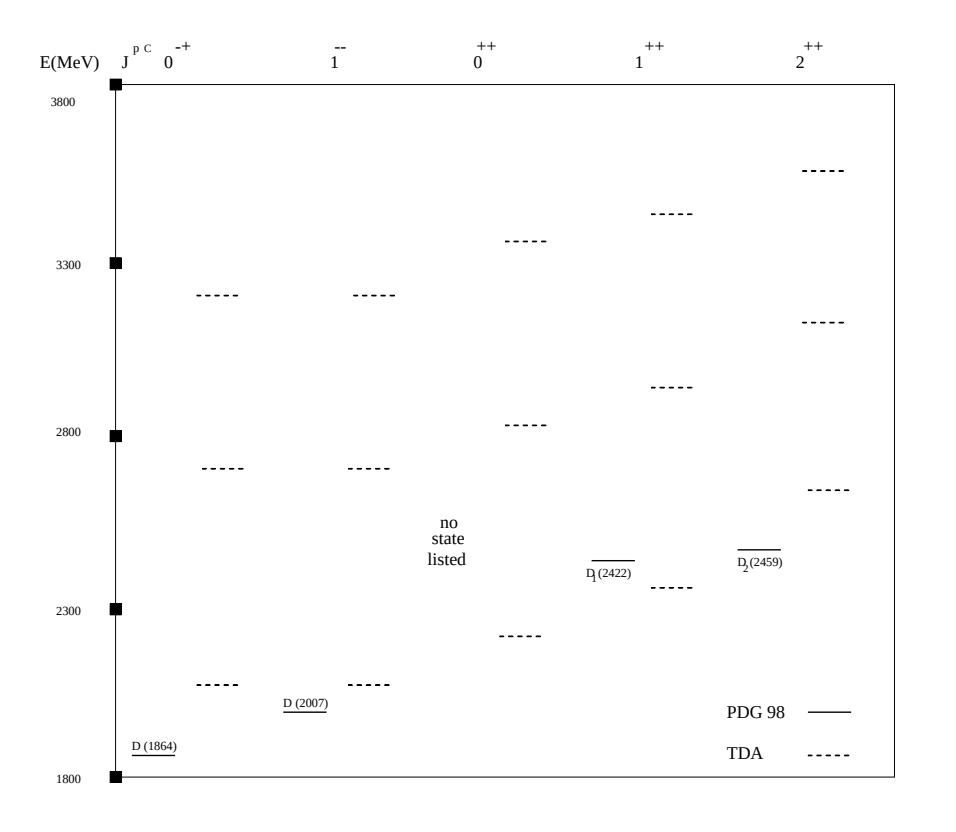

Llanes-Estrada and Cotanch, NPA 2002

D_s spectrum

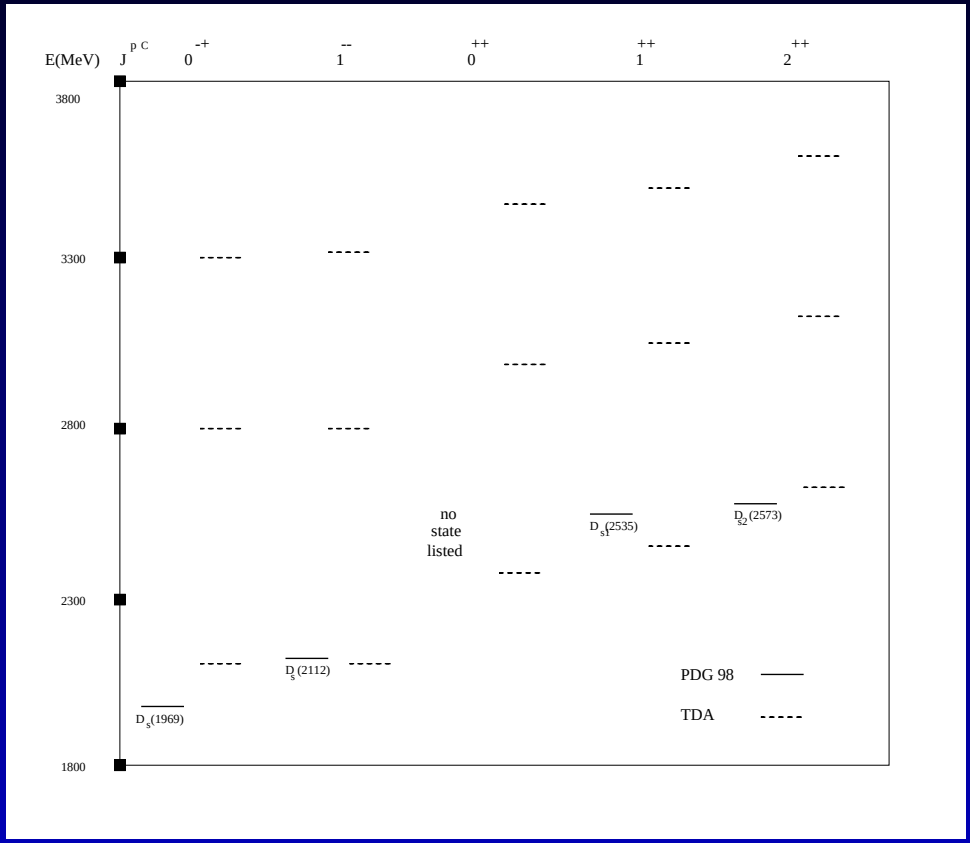

Correct counting of states, spin splittings off.

Llanes-Estrada and Cotanch, NPA 2002

Charmonium spectrum

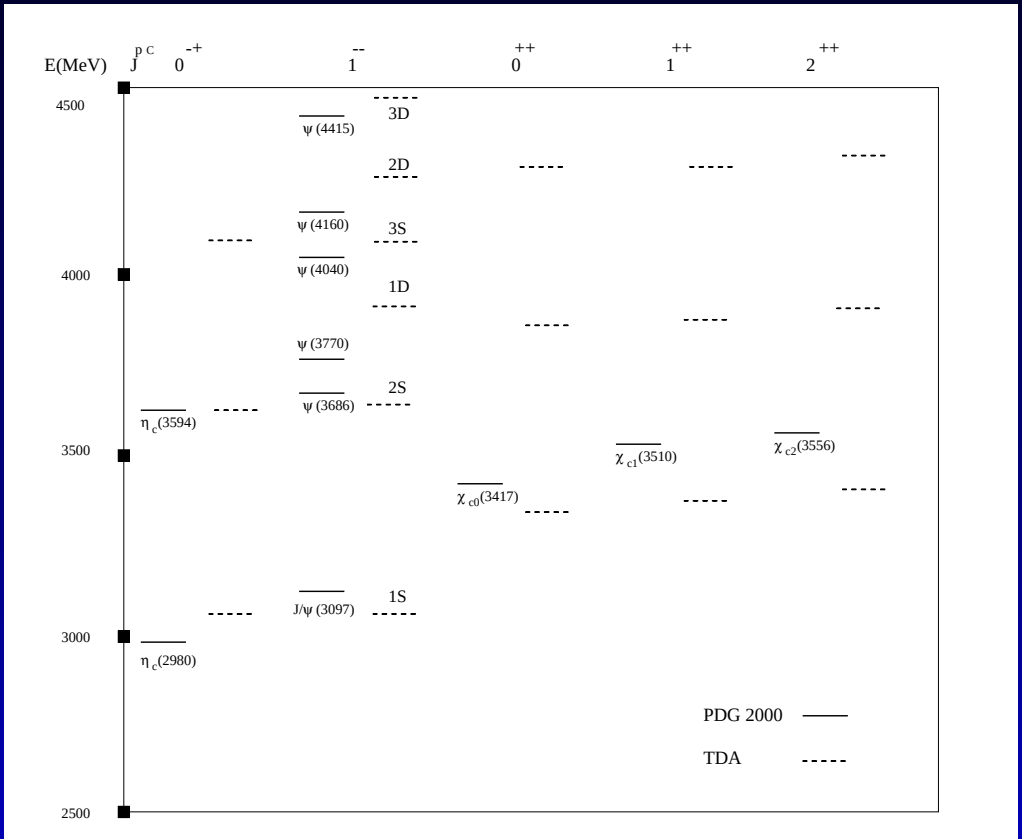

Llanes-Estrada and Cotanch, NPA 2002

Lattice Glueball spectrum

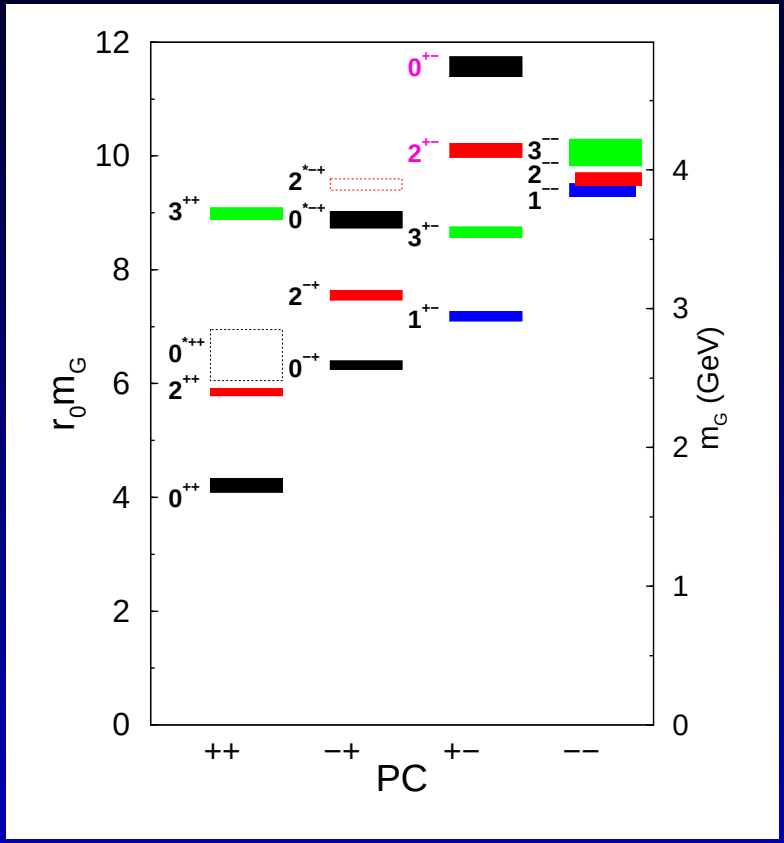

Morningstar and Peardon, PRD99

Glueballs and the pomeron

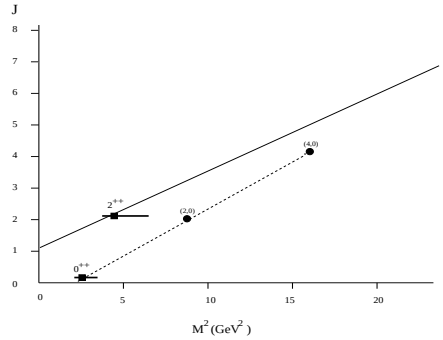

FIG. 3. Comparison of TDA (boxes) and lattice (horizontal bars) 2^{++} and 0^{++} glueballs with the Pomeron (solid line) and daughter (dashed line) Regge trajectories, respectively. The slope of the daughter trajectory is .28 GeV^{-2} and was determined by the higher ($L = 2, S = 0$) and ($L = 4, S = 0$) orbital excitations (solid circles).

14

LL-E, Szczepaniak, Bicudo, Ribeiro, Cotanch NPA2002

Inclusive glueball width

$$\Gamma = \frac{(2\pi)(4\pi)}{(2\pi)^9} \int_0^{M_G} 2\pi d\omega \int_0^{2\pi} d\phi_3 \int_0^{M_G/2} k^2$$

$$\int \int_0^{M_G/2} p_1^2 dp_1 p_3^2 dp^3 \Theta(\cos^2\theta_{p_1 k} - 1)\Theta(\cos^2\theta_{p_3 k} -$$

$$\frac{E_2}{kp_3}\frac{E_4}{kp_1}\frac{1}{(M_G - M_h)^2}\mathrm{CF}^2\mathrm{FF}^2\frac{2}{4\omega_k^2}\frac{|\phi(k)|^2}{4\pi}|S|^2(4\pi\alpha_s(k)$$

MeV	$ssg = qqg$	$ssg \simeq \frac{10}{7}uug\ (ddg)$
$\Gamma_{\mathrm{inclusive}}$	50	88
$\Gamma_{\mathrm{lightlight}}$	26	26
$\Gamma_{\mathrm{lightstrange}}$	16	33
$\Gamma_{\mathrm{strangestrange}}$	7	29

$\langle q\bar{q}g|H|q\bar{q}g\rangle$

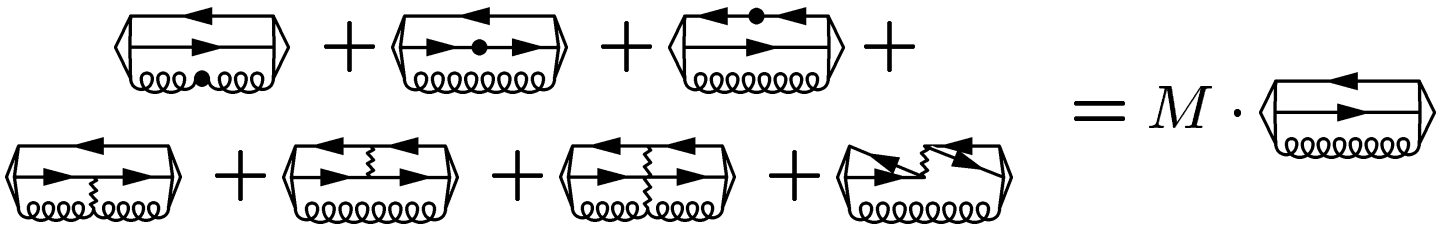

Vector charmonium hybrids

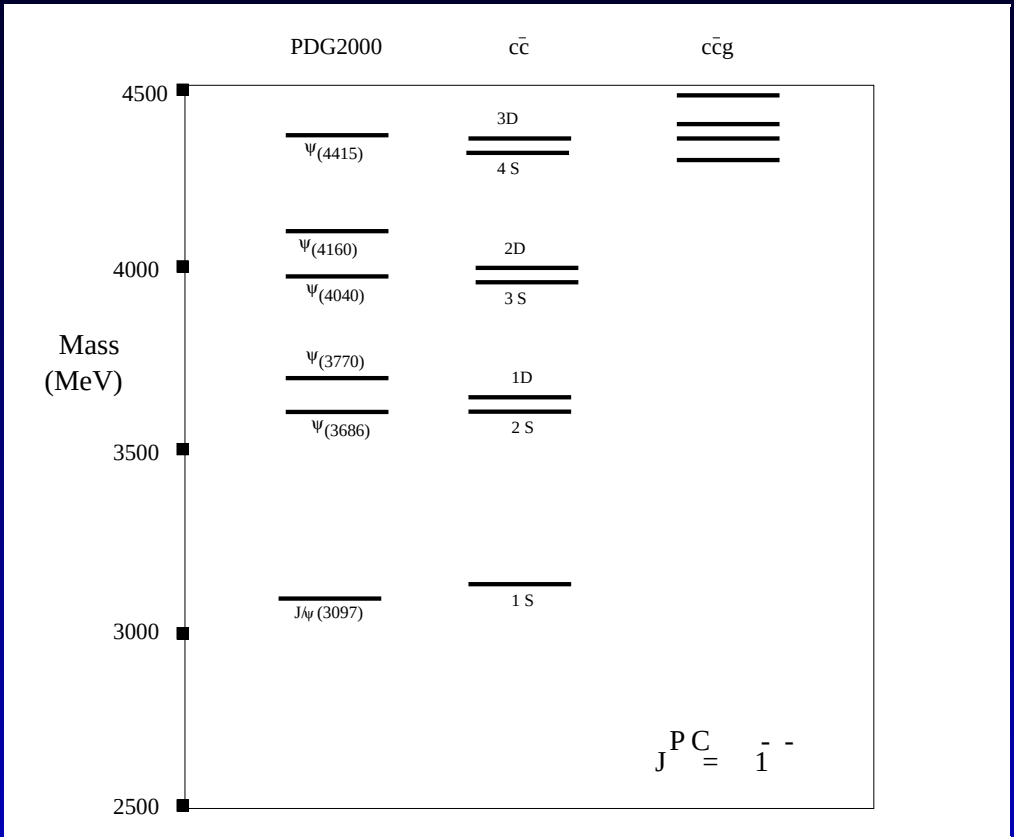

LL-E and Cotanch, PLB01

No light exotic hybrids

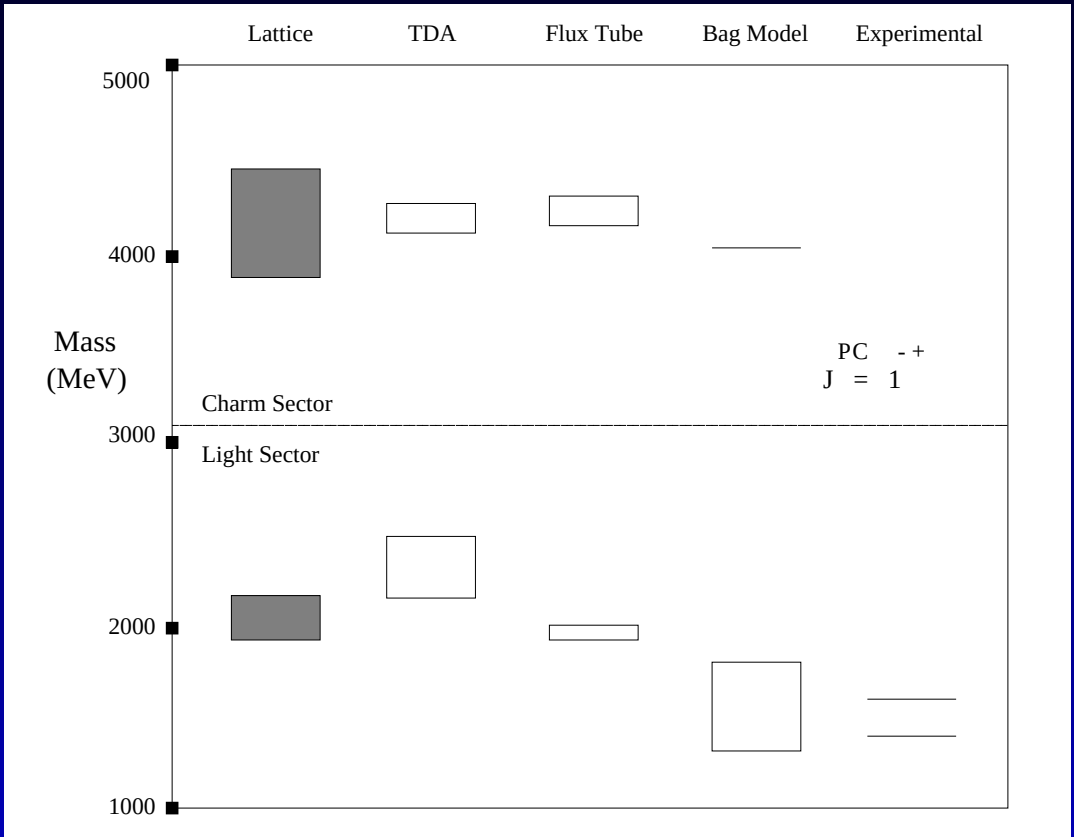

LL-E and Cotanch, PLB01

$\alpha \cdot \alpha$ kernels

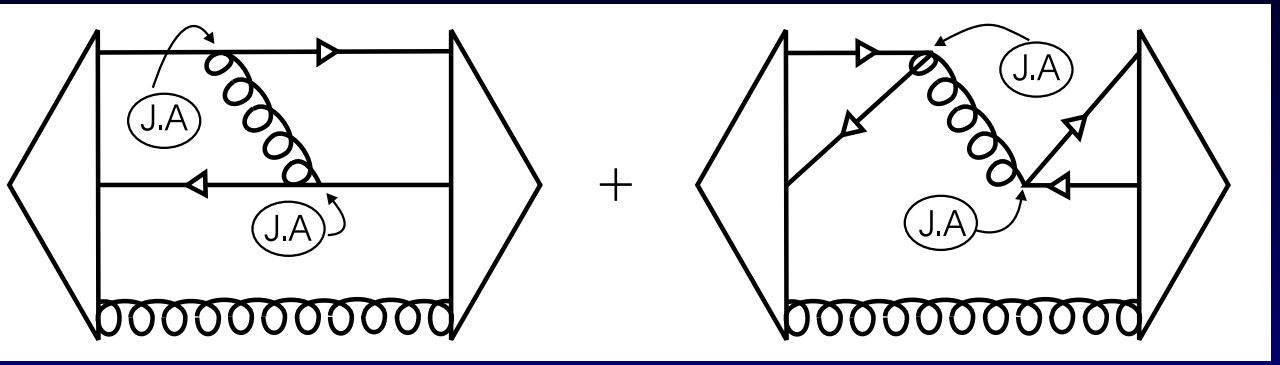

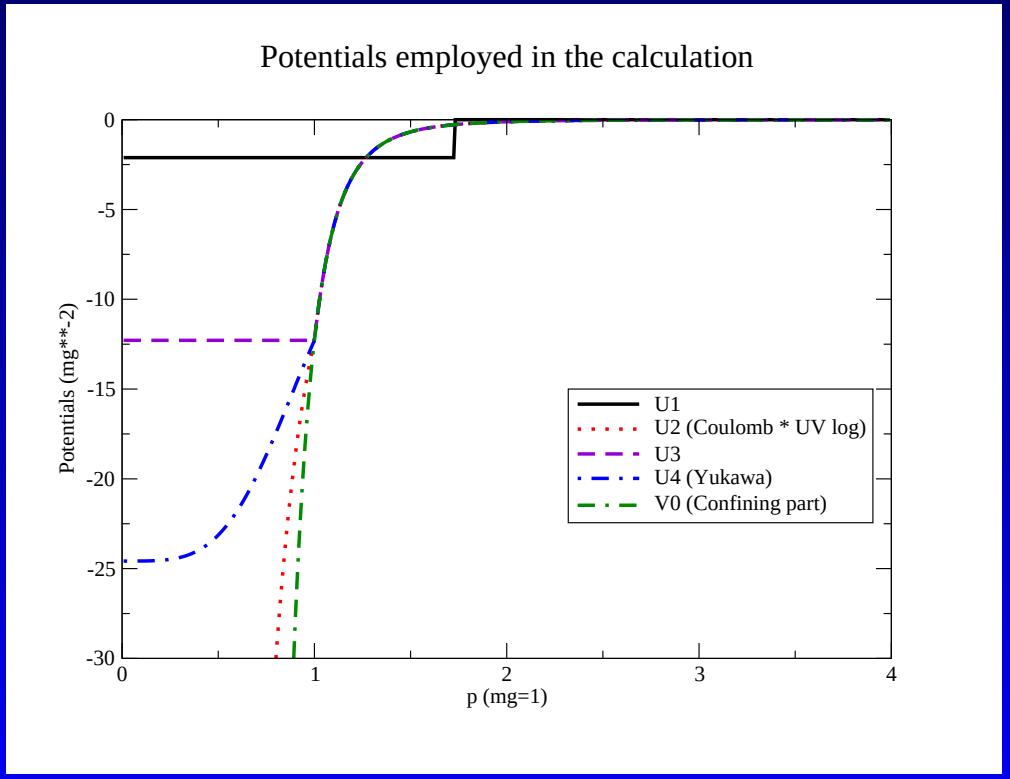

Hyperfine splittings

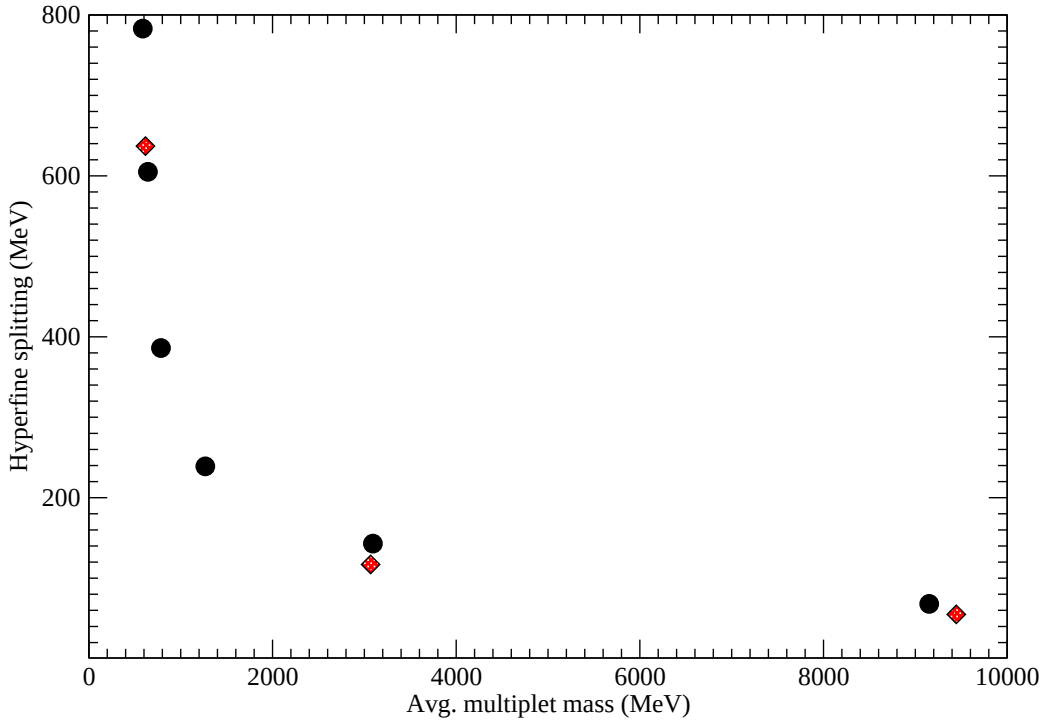

Correct prediction of η_b mass.

LL-E, Cotanch, Swanson, Szczepaniak PRC04

$\langle q\bar{q}g|H|q\bar{q}g\rangle$

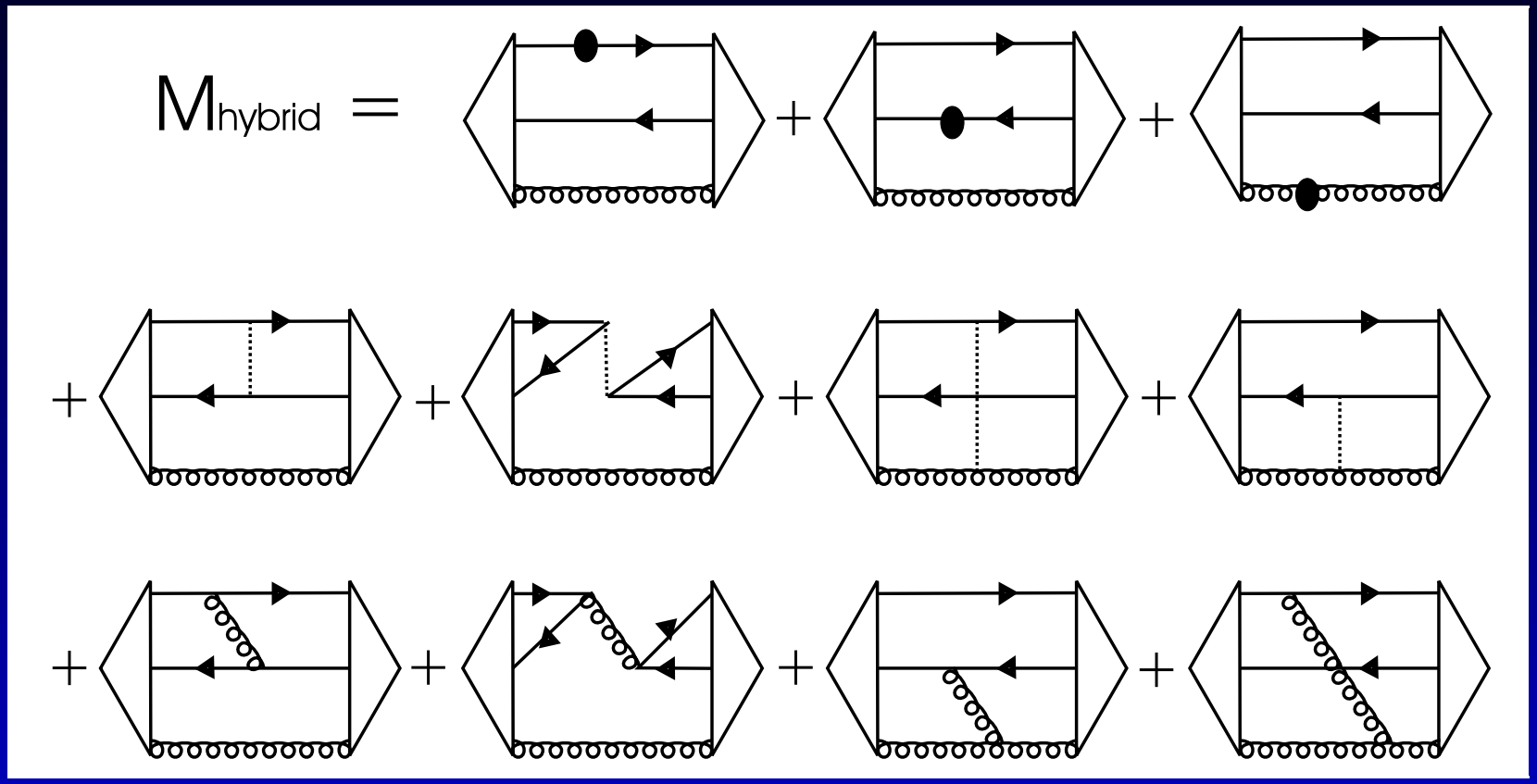

Spectrum including $\alpha \cdot \alpha$

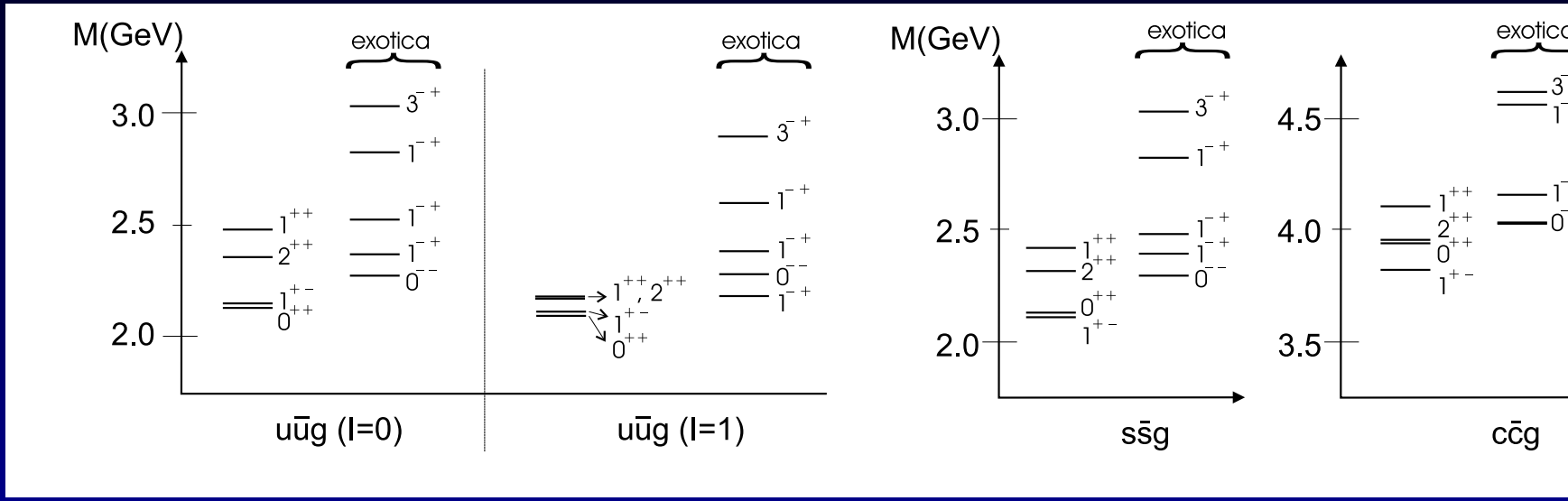

General, Cotanch and LL-E, EPJC07

Three body forces change the parity orderings (Guo's thesis 08)

Oddball Regge trajectory

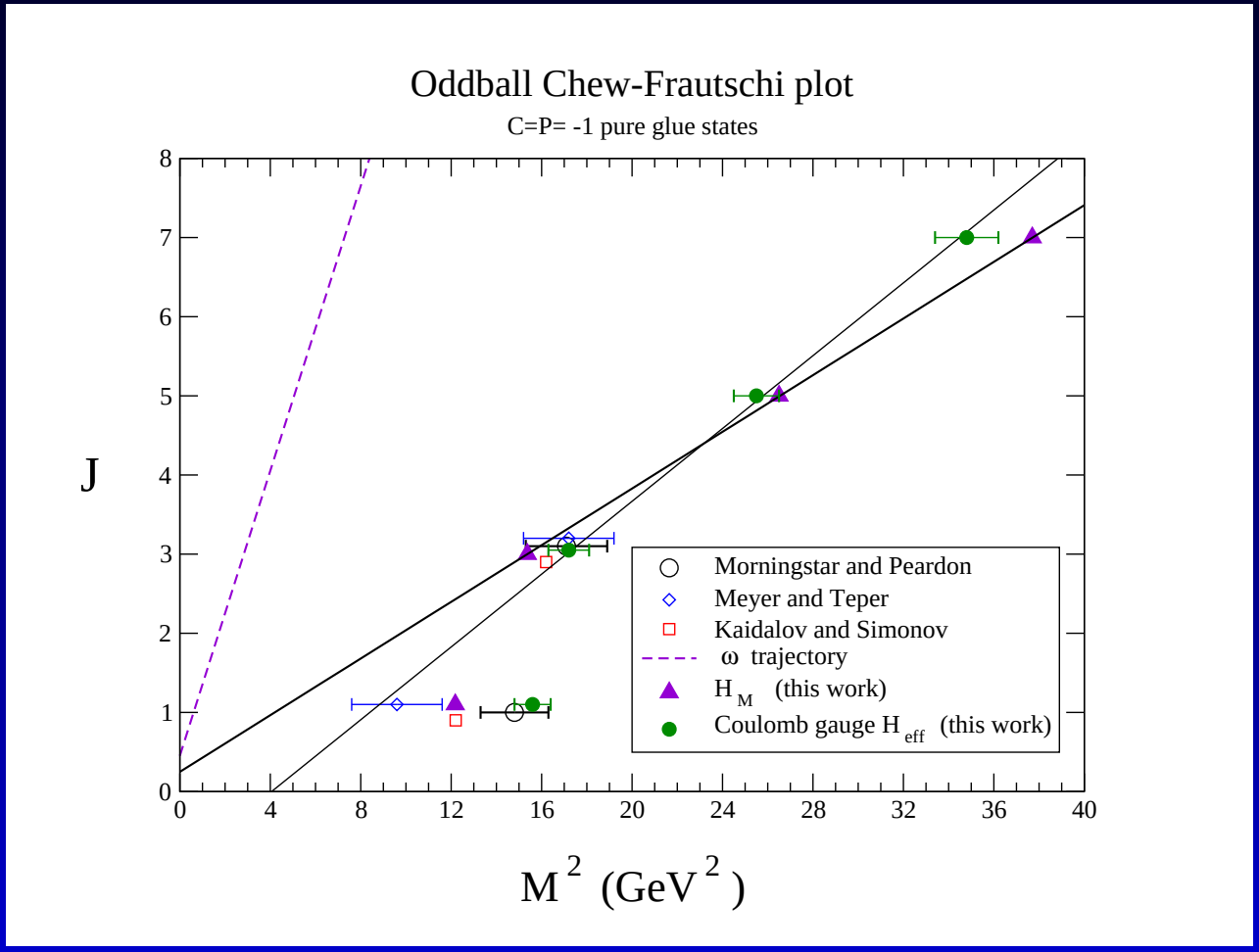

LL-E, Bicudo and Cotanch, PRL06

4q variational $\langle H \rangle$

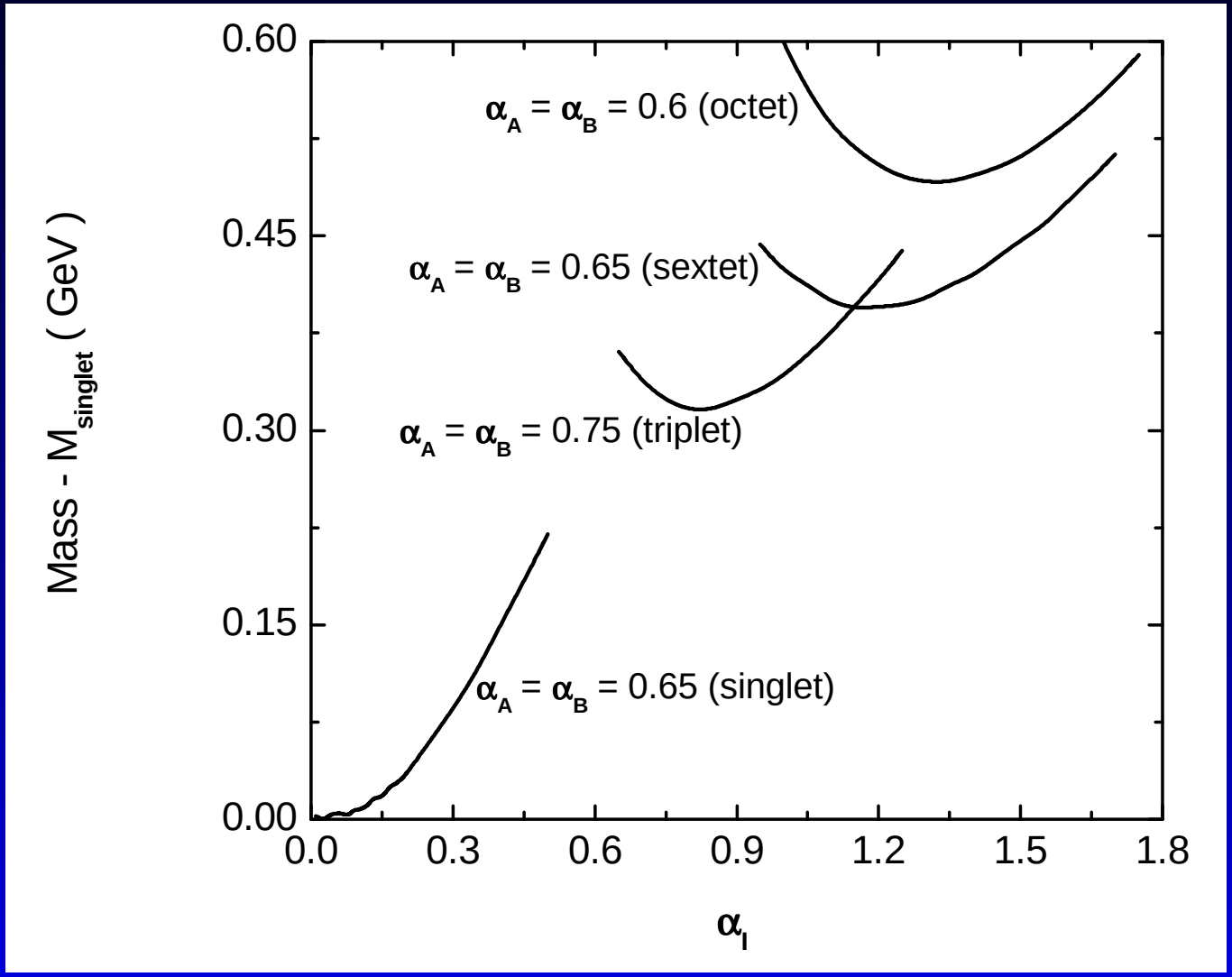

Wang, General, Cotanch and LL-E PLB07

4q variational $\langle H \rangle$

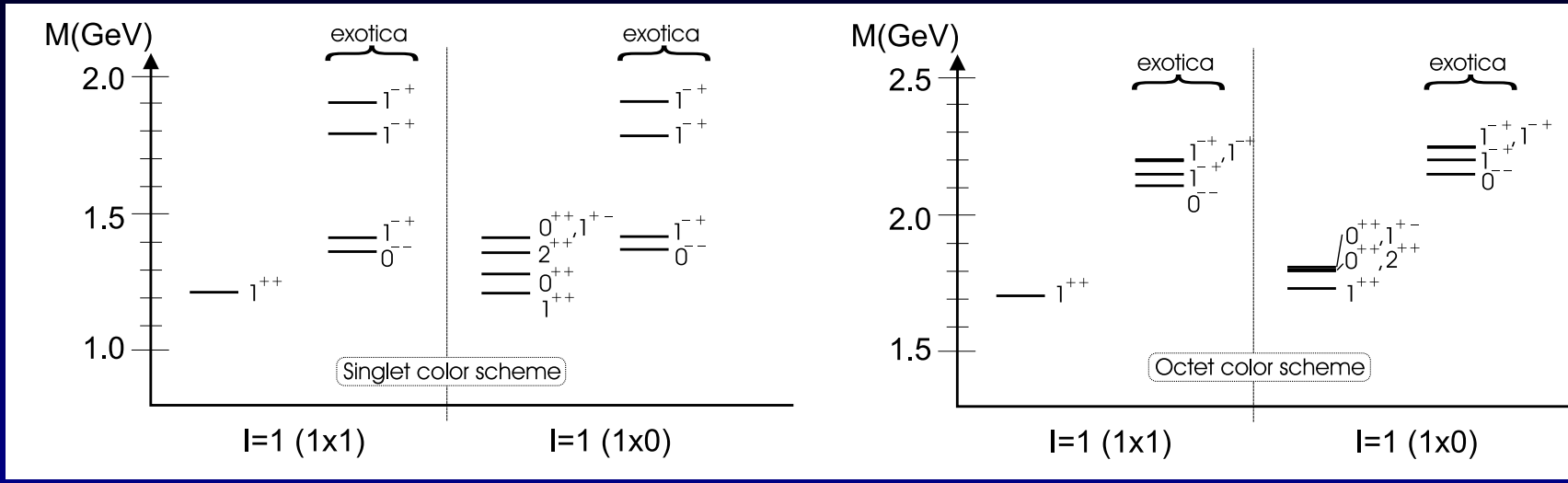

Wang, General, Cotanch and LL-E PLB07

4q variational $\langle H \rangle$

Wang, General, Cotanch and LL-E PLB07

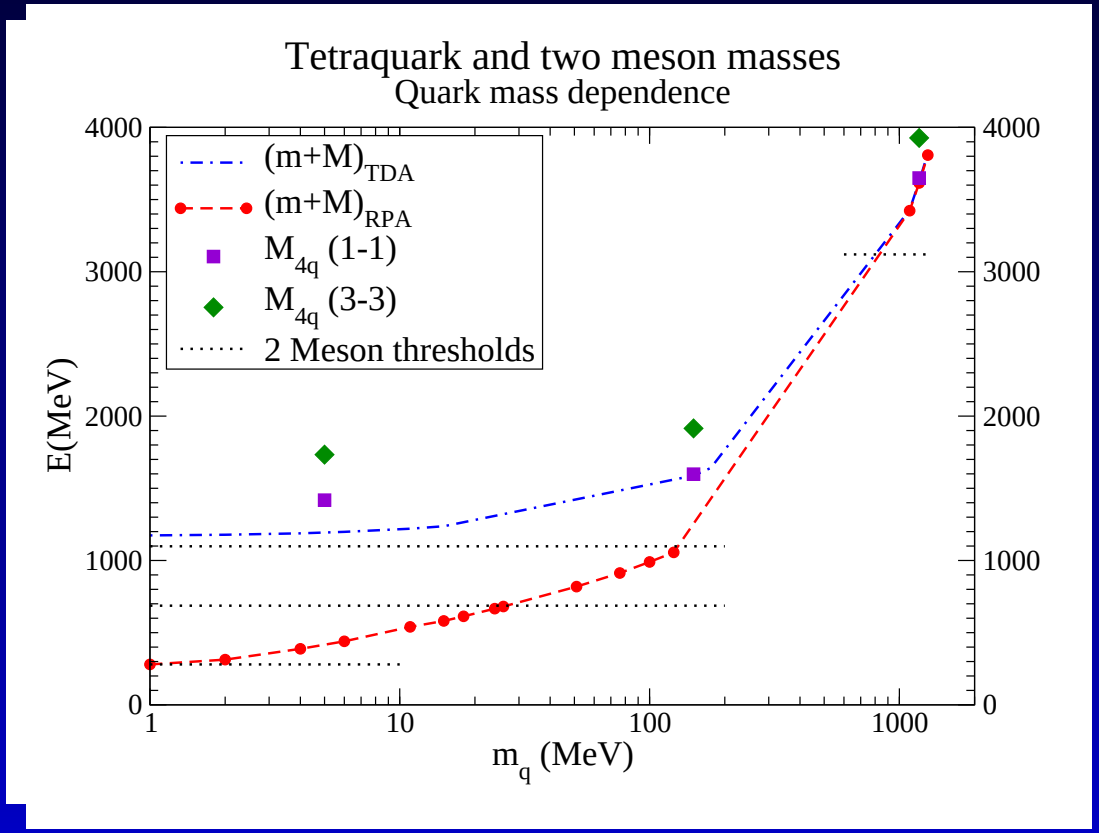

χS Wigner or Goldstone

$$[Q_5^a, \sigma_i^+] = \Theta_{ij}^a \sigma_j^-$$
$$[Q_5^a, \sigma_i^-] = \Theta_{ij}^a \sigma_j^+$$

$[Q_5^a, H] = 0$ implies $M^+ = M^-$

Alternatively

$$[Q_5^a, \sigma_i^\pm] = v_0(\pi^2)\epsilon_{abc}\pi^c \Theta_{ij}^b \sigma_j^\pm$$

Q^5 in terms of $\sin\phi(k)$

$$Q_a^5|qqq\rangle = \int \frac{d^3k}{(2\pi)^3} \sum_{\lambda\lambda' f f' c} \left(\frac{\tau^a}{2}\right)_{f f'}$$
$$\Big(\cos\phi(k)(\sigma\cdot\hat{\mathbf{k}})_{\lambda\lambda'} B^\dagger_{k\lambda f c} B_{\lambda' f' c} +$$
$$\sin\phi(k)(i\sigma_2)_{\lambda\lambda'} B^\dagger_{k\lambda f c} D^\dagger_{\lambda' f' c}\Big)\,|qqq\rangle \ .$$

Nefediev, Ribeiro, Szczepaniak 08

Chiral multiplets

3-quark chiral quartet

$$|\sigma_1^P\rangle = \sum F_{ijk}^P B_i^\dagger B_j^\dagger B_k^\dagger |$$

$$|\sigma_2^{-P}\rangle = \sum F_{ijk}^P \left(\sigma\cdot\hat{\mathbf{k}}_i B^\dagger\right)_i B_j^\dagger B_k^\dagger |$$

$$|\sigma_3^P\rangle = \sum F_{ijk}^P \left(\sigma\cdot\hat{\mathbf{k}}_i B^\dagger\right)_i \left(\sigma\cdot\hat{\mathbf{k}}_j B^\dagger\right)_j B_k^\dagger |$$

$$|\sigma_3^{-P}\rangle = \sum F_{ijk}^P \left(\sigma\cdot\hat{\mathbf{k}}_i B^\dagger\right)_i \left(\sigma\cdot\hat{\mathbf{k}}_j B^\dagger\right)_j \left(\sigma\cdot\hat{\mathbf{k}}_k B^\dagger\right)_k |$$

Chiral Symmetry à la Wigner

Van Cauteren, Bicudo, Cardoso and LL-E
PRELIMINARY

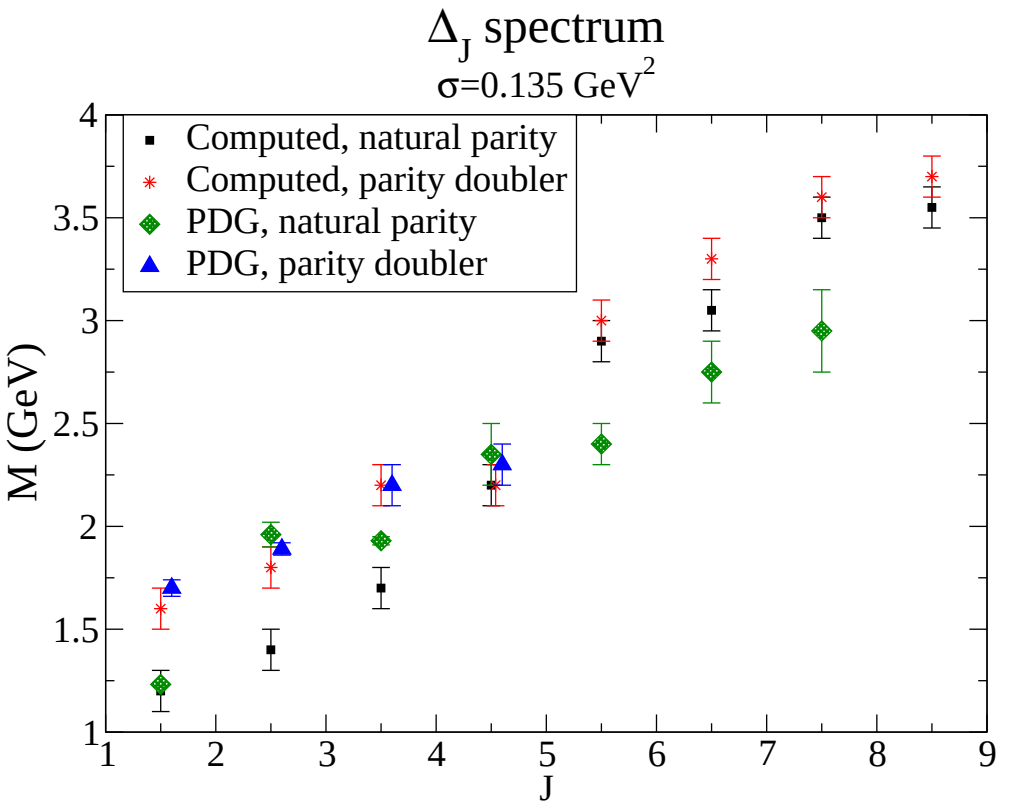

Enhance χ symmetry breaking

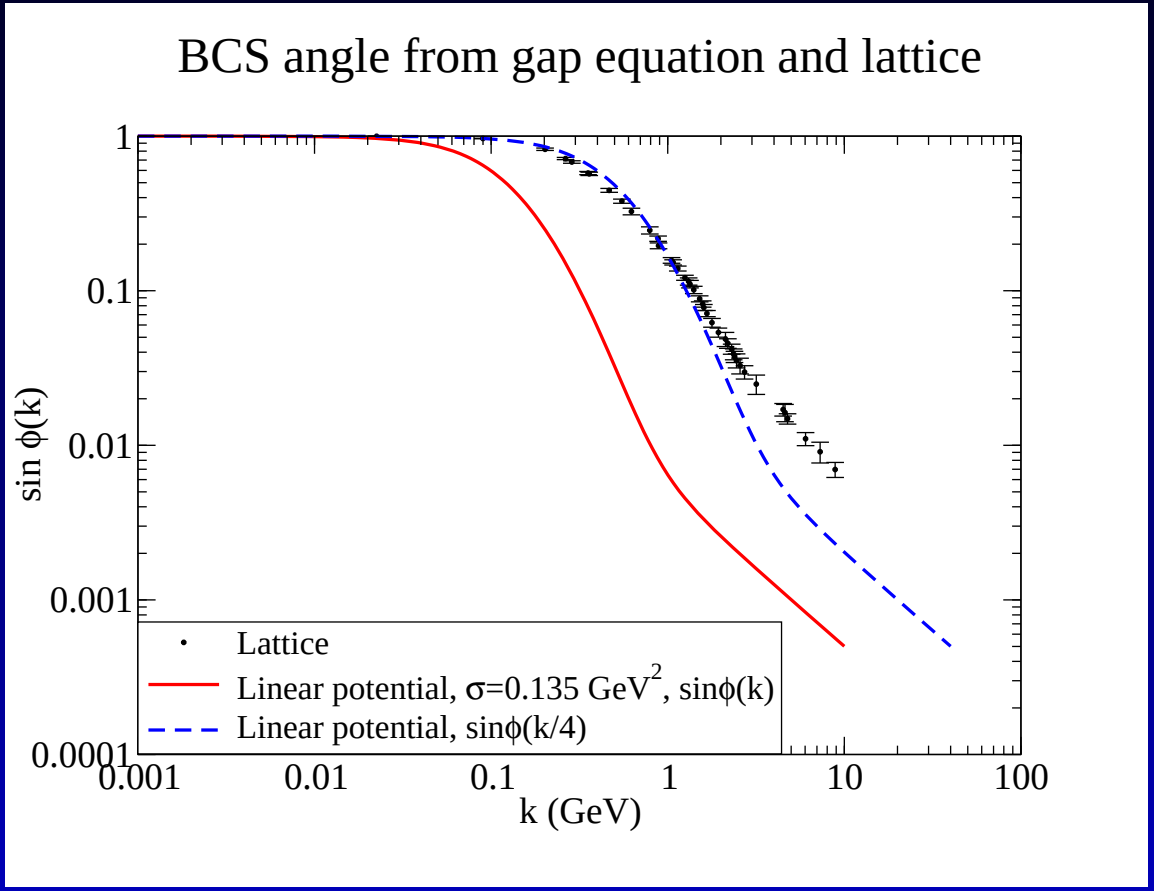

Lattice data (Landau gauge) courtesy of P. Bowman

Decreasing parity splittings

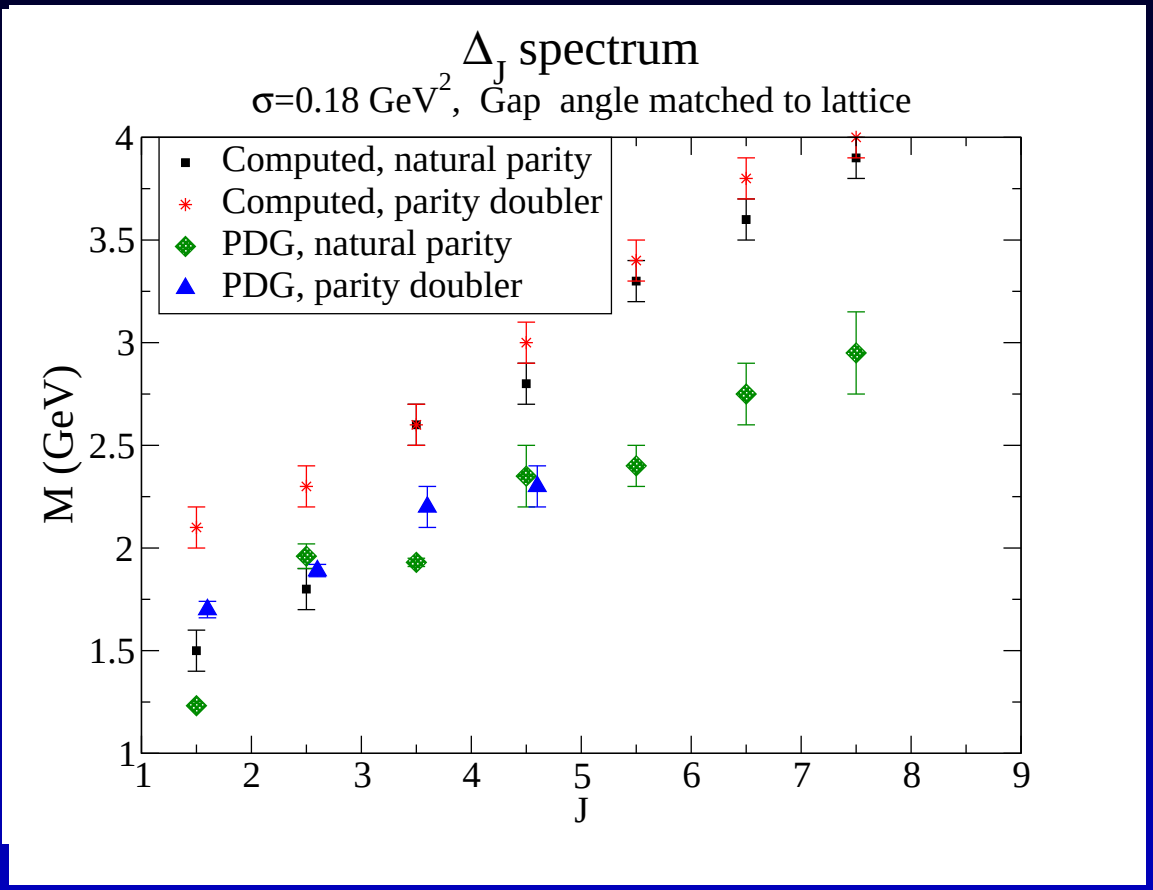

Van Cauteren, Bicudo, Cardoso and LL-E

PRELIMINARY

Chiral Symmetry à la Wigner

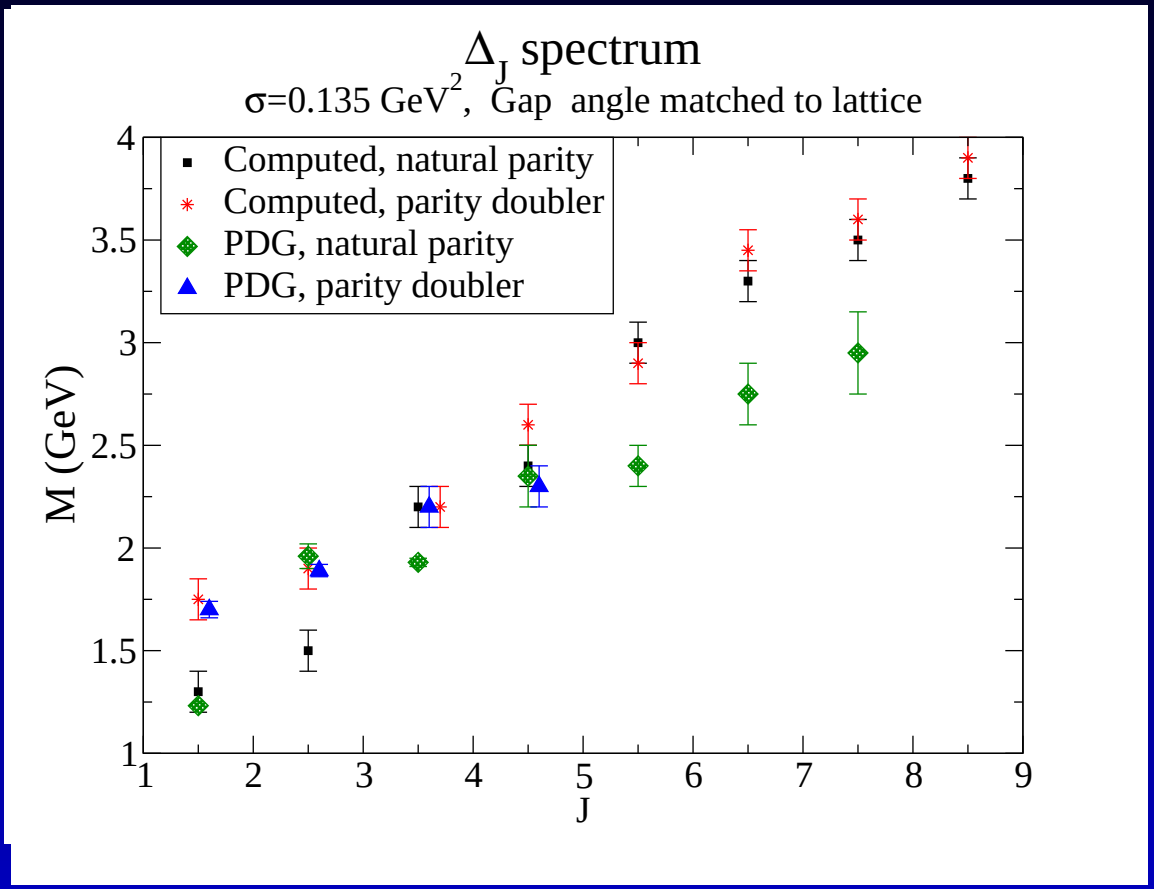

Van Cauteren, Bicudo, Cardoso and LL-E

PRELIMINARY

Decreasing parity splittings

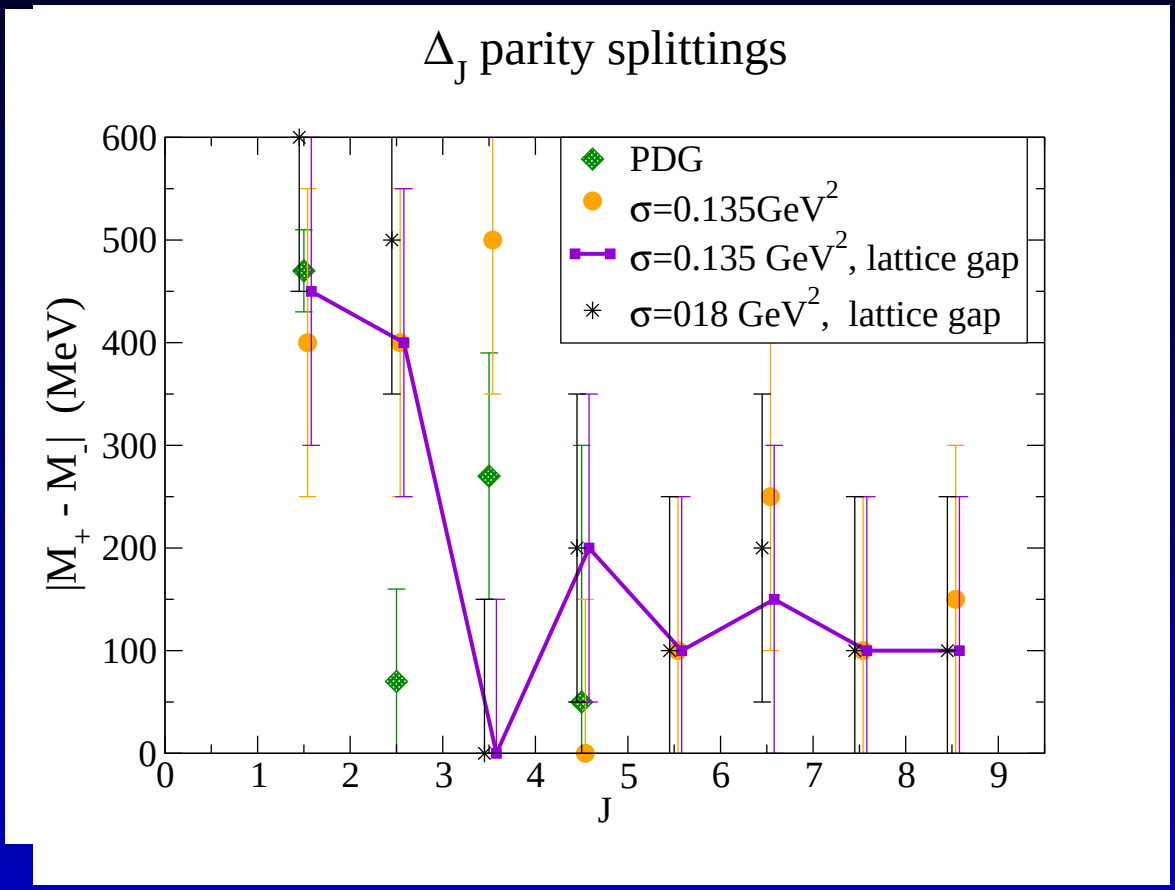

Van Cauteren, Bicudo, Cardoso and LL-E

PRELIMINARY

Coulomb gauge model lessons

- Hyperfine splittings: from OGE to chiral symmetry
- Pomeron as window to glueball spectroscopy
- Glueballs are of moderate width
- Hybrid mesons are heavier than 1.4-1.6 GeV candidates
- Oddball spectroscopy: no odderon
- Chiral symmetry restoration: Baryon quartets...